An Empirical Potential Function of α-Glycine Derived from Infrared Spectroscopic Data of D-, ^{13}C-, ^{15}N-, and ^{18}O-Labeled Species

Masato Kakihana*, Minoru Akiyama**, Tadashi Nagumo*, and Makoto Okamoto***

* Department of Chemistry, The National Defense Academy, Hashirimizu 1-10-20, Yokosuka 239, Japan.
** Department of Chemistry, Rikkyo (St. Paul's) University, Ikebukuro, Toshimaku, Tokyo 171, Japan.
*** Research Laboratory for Nuclear Reactors, Tokyo Institute of Technology, Ookayama 2-12-1, Meguroku, Tokyo 152, Japan.

Z. Naturforsch. **43a**, 774–792 (1988); received June 16, 1988

The infrared spectra (4000–100 cm^{-1}) of the α-form crystal of glycine ($NH_3^+ - CH_2 - COO^-$) and of thirteen isotopic modifications comprising D, ^{13}C, ^{15}N, and ^{18}O were measured at 80 and 290 K. Excellent resolution was reached at the low temperature. In the low temperature spectra the fine structure of the nearly degenerate NH_3 and ND_3 antisymmetric deformational modes and the CO_2-torsional bands in the vicinity of 200 cm^{-1} for each of the isotopic molecules, which in the low-frequency region are strongly overlapped by a number of lattice modes, clearly showed up. Based upon the frequency data of the 14 isotopic analogs and the precisely known structure of the molecule, a normal coordinate analysis was carried out. 307 observed frequencies were utilized to derive a new empirical valence force field reduced to a set of 50 force constants by a number of restrictive assumptions. The resulting force field reproduced the 307 frequencies with a root-mean-square deviation of 3.32 cm^{-1}. This force field emphasizes the importance of interaction force constants of the in-plane CO_2-rocking and CO_2-deformational coordinates with the CH_2-twisting coordinate, which can come form a significant deviation of this molecule from an ideal C_s-symmetry. The composition of normal vibrations from generally accepted local-symmetry coordinates is given in terms of the potential energy distribution (PED). The PED results indicate that almost all the normal modes below 1600 cm^{-1} are extensively intermixed group modes, thus precluding a simple normal vibrational decription. Interestingly the PED description for several vibrations associated with the $NH_3 - CH_2 - C$ fragment exhibits strong mixing between quasi-A' symmetric and -A'' antisymmetric coordinates with respect to a pseudo molecular symmetry (CCN) plane in this molecule.

Introduction

In a series of previous papers we have dealt with the infrared spectra and normal coordinate analyses of a set of molecules containing carboxylate groups, including acetate [1–2], pyruvate [3], and propionate [4–5]. In these investigations we have introduced approximate force fields constrained according to the criteria proposed by Hollenstein and Günthard [6], and have reported statistically well-determined sets of force constants from normal coordinate calculations. As a continuation of these studies we have investigated the infrared spectra of α-glycine.

The vibrational spectra of glycine have been the subject of a considerable number of investigations [7–19]. The interpretation of the spectra and the location of the modes are, however, controversial. Several normal coordinate calculations have been carried out for glycine and its deuterated analogs. In the early normal coordinate analyses reported by Baba et al. [20] and Suzuki et al. [7], oversimplified five and seven body models, respectively, have been employed. Dwivedi et al. [15] and Randhawa et al. [16] evaluated a Urey-Bradley force field based on the frequencies of the parent species of glycine. Considering as well the frequencies of the N-deuterated analog, Machida et al. [18] employed a modified Urey-Bradley force field and discussed the effect of hydrogen bonding in this molecule. Destrate et al. [13] reported a 39 parameter valence type force field, which was derived on the basis of the ^{15}N and ^{18}O frequency shift data as well as the data of the C- and N-deuterated analogs. However, the number of experimental frequencies used in all these earlier analyses is insufficient for determining a reliable molecular force field. In addition, except for the analy-

Reprint requests to Prof. Dr. M. Okamoto, Research Laboratory for Nuclear Reactors, Tokyo Institute of Tech. Tokyo, Japan or Dr. M. Kakihana, Department of Physics, Chalmers University of Technology, c/o Prof. L. Torell, S-412-96 Göteborg/Sweden (in Göteborg. till Sept. 1989).

0932-0784 / 88 / 0800-0774 $ 01.30/0. – Please order a reprint rather than making your own copy.

sis given by Machida et al. [18], all these previous computations are based upon the simplifying assumption that both the amino and methylene groups in glycine have tetrahedral configuration, which is far from the actual structure of this molecule [21–22].

The present work has two objectives: (i) to obtain firm assignments for all fundamentals; (ii) to provide data for a more reliable determination of the force field of glycine. The present vibrational analysis is based upon an extensive set of empirical data, inlcuding infrared fundamental frequencies as measured at liquid nitrogen temperature, of 14 isotopic species: $NH_3^+CH_2COO^-$ (parent, d_0), $NH_3^+CH_2{}^{13}COO^-$ (1-^{13}C), $NH_3^+{}^{13}CH_2COO^-$ (2-^{13}C), $^{15}NH_3^+CH_2COO^-$, $NH_3^+CH_2C^{18}O^{18}O^-$, $NH_3^+{}^{13}CH_2{}^{13}COO^-$, $^{15}NH_3^+{}^{13}CH_2COO^-$, $NH_3^+CD_2COO^-$ (C-d_2), $NH_3^+{}^{13}CD_2{}^{13}COO^-$, $ND_3^+CH_2COO^-$ (N-d_3), $^{15}ND_3^+CH_2COO^-$, $ND_3^+CH_2{}^{13}COO^-$, $ND_3^+CD_2COO^-$ (d_5), and $ND_3^+{}^{13}CD_2{}^{13}COO^-$.

In Sect. A, some arguments about the vibrational assignment are briefly advanced in terms of qualitative empirical rules for group vibrations in combination with the isotopic shifts of the fundamentals. The normal coordinate analysis is reported in Section B. A large number of frequency data over the 14 isotopic species as well as the precise structural parameters reported by Jönsson et al. [21] are now used to allow a constrained potential function of glycine to be determined. Our calculation is based upon an isolated glycine molecule, i.e. only intramolecular terms are mathematically taken into consideration and strain from the intermolecular forces amongst the glycine molecules is neglected. Although the observed frequency data are rather comprehensive, a complete intramolecular force field could not be determined. The set of intramolecular force constants was therefore reduced by a number of restrictive assumptions, which are expected to be acceptable from a physical point of view. The approximate intramolecular force field thus constructed consists of 17 diagonal and 33 off-diagonal terms, which were entered into a generally accepted force constant refinement routine to minimize the error between the observed and calculated frequencies. It will be finally shown that the inclusion of data from the heavy atom isotope (^{13}C, ^{15}N, ^{18}O) modifications allowed us to estimate, with good accuracy, a number of relevant interaction force constants associated with the C–C, C–N, and C–O skeletons in this molecule.

Experimental

Potassium bromide, paraffin liquid, and normal gylcine were obtained commercially (suprapur reagents, E. Merck Co. Ltd., Darmstadt). The ^{13}C-, ^{15}N-, ^{18}O-, and C-d_2-labeled modifications of glycine were purchased from Merck Sharp and Dohme Canada Ltd. with 90–99% isotopic purity. The N-deuterated derivatives were prepared by direct exchange with 99.7% D_2O; the initial non N-deuterated species were dissolved in D_2O and kept at room temperature for a few minutes. Then the crystals were obtained from evaporating the water. This procedure was repeated three times. α-form crystals of glycine were obtained by rapid evaporation of hot aqueous solutions. The infrared spectra were recorded on a Bruker IFS-113v FT-IR spectrometer in the 4000–100 cm^{-1} region with a resolution of 0.5 cm^{-1}. A liquid nitrogen cryostat equipped with KRS-5 or polyethylene windows, Model CF-1104 (Oxford Instrument), was used for the low-temperature experiments. Samples for the infrared spectra of N-deuterated species were prepared as nujol (paraffin liquid) mulls between KBr or polyethylene windows, and the records for the remaining samples were made with KBr pellets in the mid infrared range (4000–500 cm^{-1}) and with nujol mulls between polyethylene windows in the far-infrared region (500–100 cm^{-1}).

Results and Discussion

A. Vibrational Assignments

The frequencies observed at 80 K for the parent and its thirteen isotopic modifications are listed in Tables 1–6, along with their proposed assignments. Fine structures of complex overlapping regions were revealed by measuring the spectra at 80 K, making it possible to locate the fundamental frequencies without ambiguity. This advantage of measuring spectra at the low temperature is demonstrated for the parent species in Fig. 1, covering two interesting spectral regions, 1700–1250 and 600–100 cm^{-1}. The ν_6, ν_7, ν_{13}, ν_{21}, and ν_{24} bands, which were hardly discernible in the room temperature sprectrum, clearly showed up in the low temperature spectrum. Low temperature spectra are used throughout in this paper for the identification of absorption peaks.

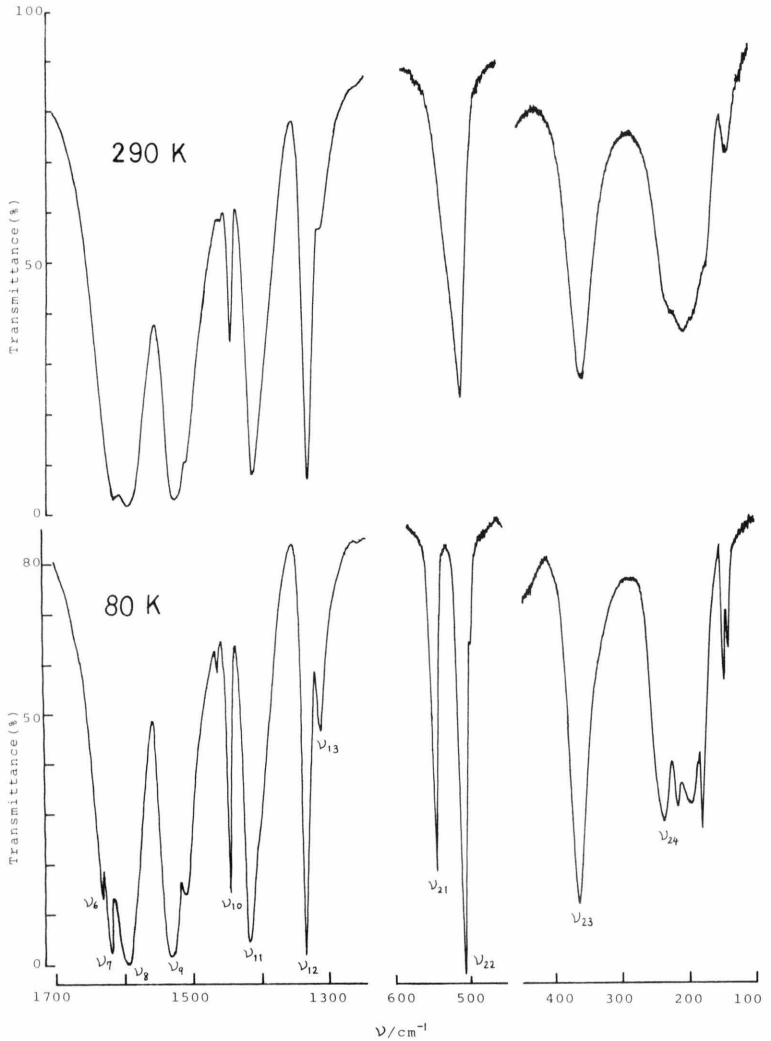

Fig. 1. Comparison of the IR spectrum of the α-form crystal of $NH_3^+CH_2COO^-$ measured at 80 K (below) with that at 290 K (above).

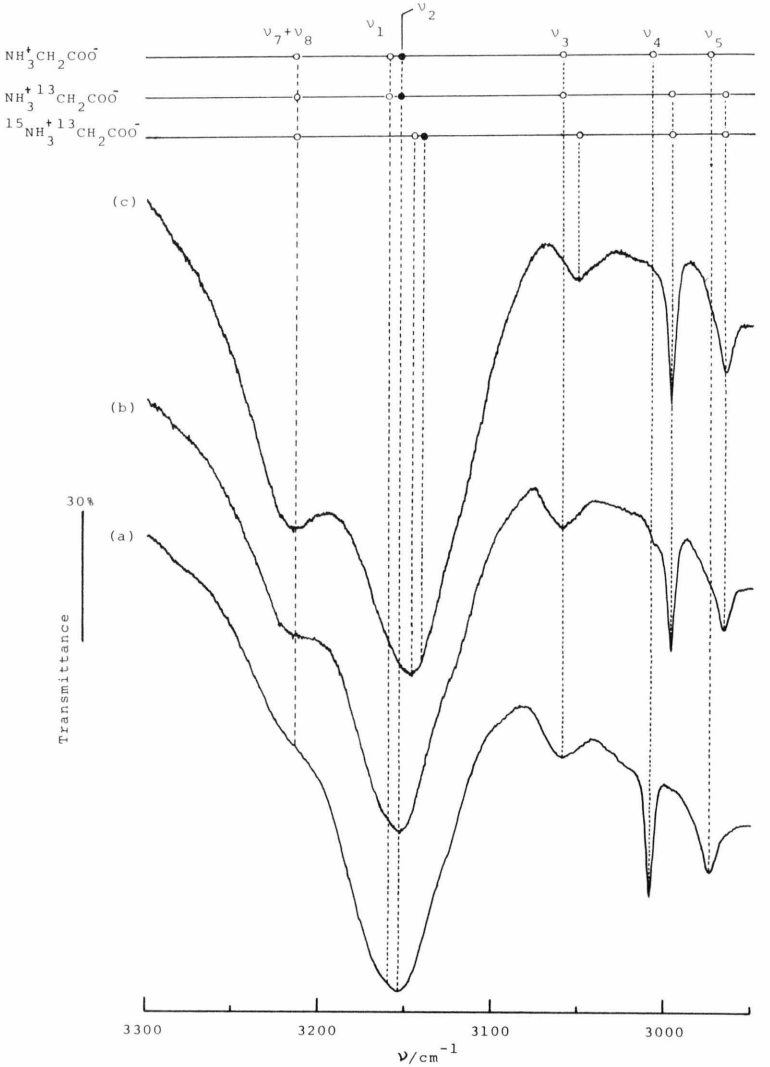

Fig. 2. N−H and C−H stretching region of the IR spectra of α-$NH_3^+CH_2COO^-$ (a), α-$NH_3^+CH_2{}^{13}COO^-$ (b), and α-$^{15}NH_3^+CH_2COO^-$ (c) at 80 K. The final interpretation for the band assignments is indicated as symbols ν_i at the top of the spectra.

Table 1. Observed and calculated frequencies for $NH_3^+CH_2COO^-$ (α-form) at 80 K.

Assignment		ν/cm^{-1}		Potential energy distribution (PED)[a]
		obs.	calc.	
FR[b]	$\nu_7+\nu_8$	3210[c]		
	ν_1	overlap	3159.3	87 $\nu_{as}(NH_3)$, 12 $\nu'_{as}(NH_3)$
	ν_2	3152.2	3153.6	87 $\nu'_{as}(NH_3)$ 12 $\nu_{as}(NH_3)$
	ν_3	3058.2	3058.3	100 $\nu_s(NH_3)$
	ν_4	3008.5	3008.6	99 $\nu_{as}(CH_2)$
	ν_5	2972.8	2972.8	99 $\nu_s(CH_2)$
	ν_6	1633.9	1634.1	48 $\delta'_{as}(NH_3)$, 45 $\delta_{as}(NH_3)$
	ν_7	1617.5	1615.8	51 $\delta_{as}(NH_3)$, 36 $\delta'_{as}(NH_3)$
	ν_8	1596.7	1597.2	70 $\nu_{as}(CO_2)$, 19 $\gamma_{in}(CO_2)$, 12 $\delta'_{as}(NH_3)$
	ν_9	1532.6	1533.1	85 $\delta_s(NH_3)$, 11 $\nu_{as}(CO_2)$
		1507.0[d,e]		
	ν_{10}	1445.9	1443.9	85 $\delta(CH_2)$
	ν_{11}	1416.6	1418.9	44 $\nu_s(CO_2)$, 24 ν(CC), 20 $\gamma_w(CH_2)$
	ν_{12}	1336.8	1335.8	22 $\nu_s(CO_2)$, 18 $\gamma_w(CH_2)$, 16 $\gamma_t(CH_2)$, 14 $\pi(NH_3)$
	ν_{13}	1315.3	1317.7	57 $\gamma_w(CH_2)$, 13 $\gamma_t(CH_2)$
	ν_{14}	1138.4	1139.4	56 $\gamma_{in}(NH_3)$, 13 δ(CCN)
	ν_{15}	1119.0	1119.5	22 $\pi(NH_3)$, 21 $\gamma_{in}(NH_3)$, 16 $\gamma_r(CH_2)$, 16 $\tau(NH_3)$, 11 $\gamma_t(CH_2)$
	ν_{16}	1036.9	1037.6	54 ν(CN), 15 $\gamma_{in}(CO_2)$, 10 $\nu_s(CO_2)$
	ν_{17}	918.9	917.7	26 $\pi(NH_3)$, 17 $\gamma_r(CH_2)$, 16 $\tau(NH_3)$, 10 $\delta(CO_2)$, 10 $\tau(CO_2)$
	ν_{18}	897.2	896.2	20 ν(CC), 20 $\pi(CO_2)$, 16 $\delta(CO_2)$
	ν_{19}	703.6	702.8	33 $\pi(CO_2)$, 25 ν(CN), 21 $\gamma_t(CH_2)$, 17 $\gamma_{in}(CO_2)$, 15 $\delta(CO_2)$, 15 δ(CCN)
	ν_{20}	613.2	615.1	78 $\pi(CO_2)$, 59 $\gamma_t(CH_2)$, 29 $\gamma_{in}(CO_2)$, 19 δ(CCN), 12 ν(CC)
	ν_{21}	544.7	543.3	41 $\tau(NH_3)$, 27 $\gamma_r(CH_2)$, 13 δ(CCN), 11 $\delta(CO_2)$
	ν_{22}	506.9	506.9	45 $\gamma_{in}(CO_2)$, 21 $\delta(CO_2)$, 14 $\gamma_t(NH_3)$, 13 $\tau(CO_2)$, 12 $\gamma_w(CH_2)$, 12 $\tau(NH_3)$, 11 δ(CCN)
	ν_{23}	364.3	362.7	43 δ(CCN), 33 $\delta(CO_2)$, 18 ν(CC), 12 $\nu_s(CO_2)$
	ν_{24}	238.4	237.1	59 $\tau(CO_2)$, 41 $\gamma_t(CH_2)$, 25 $\gamma_r(CH_2)$, 12 $\pi(CO_2)$, 12 $\pi(NH_3)$, 10 $\gamma_{in}(CO_2)$

[a] PED is given as values of $100 \times F_s(i,i) \times L_s^2(i,a)/\lambda_a$, where F_s, L_s, and λ_a are diagonal force constants, eigen vectors and eigen values for GF-matrix, respectively, within the framework of symmetry coordinate space. Contributions smaller than 10% are omitted. — [b] FR = Fermi resonance. — [c] Shoulder.
[d] Minor components resulting from factor-group splittings.
[e] Not used in the refinement procedure for the determination of the empirical force field.

An initial assignment of the fundamentals was carried out on the basis of the qualitative empirical rules available [23] and of comparisons with the earlier vibrational assignments [9, 13, 18] of glycine as well as of structurally related molecules such as sodium propionate [5] and alanine [24–25]. The observed heavy atom isotope (^{13}C, ^{15}N, ^{18}O) shifts of the fundamentals were quite useful to confirm or to revise the previous vibrational assignments. However, because of the general asymmetry of this molecule, it is very likely that many of normal modes are highly complex mixtures of group modes, so that the application of the empirical approach to establish the band assignments is restricted to specific regions in which the vibrations are good group modes. In what follows, a few remarks are made only on noteworthy or doubtful aspects of the vibrational assignments.

1. NH(D)- and CH(D) Stretching Region

In the region of 3300–2950 cm^{-1} for the parent species, a total of 5 fundamentals are expected to occur; three of them are due to NH_3 stretching modes, and the other ones to CH_2 stretching vibrations. An expanded section of the spectrum of the parent species is shown in Figure 2a. Going from the high frequency side to the lower frequency side, one finds a strong and broad band (ν_1/ν_2) with a shoulder ($\nu_7+\nu_8$), a weak band (ν_3), a sharp band (ν_4), and a

Table 2. Observed and calculated frequencies for $NH_3^+CD_2COO^-$ and $NH_3^+{}^{13}CD_2{}^{13}COO^-$ (α-form) at 80 K.

Assignment		$NH_3^+CD_2COO^-$ ν/cm^{-1}		$NH_3^+{}^{13}CD_2{}^{13}COO^-$ ν/cm^{-1}		Potential energy distribution (PED)[a]
		obs.	calc.	obs.	calc.	
FR[b]	$\nu_7+\nu_8$	3210[c]		3210[c]		
FR[b]	ν_1	overlap	3159.1	overlap	3159.1	88 $\nu_{as}(NH_3)$, 12 $\nu'_{as}(NH_3)$
FR[b]	ν_2	3150.8	3153.5	3155.4	3153.5	88 $\nu'_{as}(NH_3)$, 12 $\nu_{as}(NH_3)$
	ν_3	not obs.	3058.2	3058.0	3058.3	100 $\nu_s(NH_3)$
FR[b]	ν_4	2257.3[d]	2245.8	2238.3[d]	2227.6	97 $\nu_{as}(CD_2)$
FR[b]	$2\nu_{13}$	2233.9		2198.5		
FR[b]	ν_5	2164.5[d]	2177.4	2145.9[d]	2165.3	97 $\nu_s(CD_2)$
FR[b]	$\nu_7+\nu_{21}$	2145.9		overlap		
FR[b]	ν_6	1643.7[d]	1633.3	1638.2[d]	1633.2	51 $\delta'_{as}(NH_3)$, 43 $\delta_{as}(NH_3)$
FR[b]	ν_7	1619.6[d]	1614.3	1614.8	1613.4	56 $\delta_{as}(NH_3)$, 39 $\delta'_{as}(NH_3)$
FR[b]	$2\nu_{18}$	1606.1		1595[c]		
	ν_8	1587.2	1582.7	1560.8	1554.1	79 $\nu_{as}(CO_2)$, 21 $\gamma_{in}(CO_2)$, 11 $\delta_s(NH_3)$
	ν_9	1525.4	1531.6	1522.7	1516.3	81 $\delta_s(NH_3)$, 18 $\nu_{as}(CO_2)$
		1503.3[d, e]		1489.0[d, e]		
	ν_{10}	1407.2[f]	1406.1	1372.0	1370.6	68 $\nu_s(CO_2)$, 29 ν(CC), 13 $\delta(CO_2)$
				1393.3[d, e]		
	ν_{11}	1215.9	1210.4	1206.9	1205.1	58 $\pi(NH_3)$
	ν_{12}	1188.3	1188.0	1183.6	1174.7	36 $\gamma_{in}(NH_3)$, 27 $\gamma_w(CD_2)$, 19 ν(CN), 13 $\nu_s(CO_2)$
	ν_{13}	1113.4	1108.5	1092.2	1090.0	42 $\gamma_{in}(NH_3)$, 32 ν(CN), 19 δ(CCN), 12 $\gamma_{in}(CO_2)$
FR[b]	$2\nu_{21}$	1060.3		1052.8		
FR[b]	ν_{14}	1044.2	1036.8	1038.9	1032.2	65 $\delta(CD_2)$, 15 $\gamma_w(CD_2)$
	ν_{15}	928.4	931.3	919.3	922.7	24 $\pi(CO_2)$, 15 $\pi(NH_3)$, 14 $\gamma_t(CD_2)$, 13 $\tau(NH_3)$
		934.5[d, e]		913.0[d, e]		
	ν_{16}	911.1	912.2	907.5	906.2	23 $\gamma_w(CD_2)$, 22 $\delta(CO_2)$, 13 ν(CC)
	ν_{17}	873.2	872.1	864.9	863.6	17 $\gamma_w(CD_2)$, 12 ν(CN), 12 ν(CC), 12 $\gamma_{in}(NH_3)$, 10 $\gamma_{in}(CO_2)$
	ν_{18}	802.8	795.6	796.8	789.1	43 $\tau(NH_3)$, 28 $\gamma_r(CD_2)$., 26 $\pi(CO_2)$
	ν_{19}	675.0	674.7	666.0	670.0	33 $\gamma_{in}(CO_2)$, 26 ν(CN), 18 δ(CCN), 11 $\delta(CO_2)$, 11 $\gamma_t(CD_2)$
	ν_{20}	566.6	560.7	not obs.	551.0	51 $\pi(CO_2)$, 50 $\gamma_t(CD_2)$, 26 δ(CCN), 20 ν(CC), 15 $\delta(CO_2)$
	ν_{21}	529.6	523.9	528.4	518.6	33 $\gamma_r(CD_2)$, 29 $\tau(NH_3)$, 25 $\gamma_t(CD_2)$, 14 $\gamma_{in}(CO_2)$, 11 δ(CCN), 11 $\delta(CO_2)$
	ν_{22}	472.4	470.3	471.8	467.6	45 $\gamma_{in}(CO_2)$, 41 $\gamma_t(CD_2)$, 25 $\tau(CO_2)$, 18 $\gamma_r(CD_2)$, 17 $\pi(CO_2)$, 12 $\pi(NH_3)$, 11 $\delta(CO_2)$, 10 $\gamma_w(CD_2)$
	ν_{23}	359.0	357.9	358.0	357.0	41 δ(CCN), 35 $\delta(CO_2)$, 18 ν(CC), 13 $\nu_s(CO_2)$
	ν_{24}	233.6	229.6	—[g]	227.9	62 $\tau(CO_2)$, 41 $\gamma_t(CD_2)$, 21 $\gamma_r(CD_2)$, 11 $\pi(CO_2)$, 11 $\pi(NH_3)$

[a] PED is given as values of $100 \times F_s(i, i) \times L_s^2(i, a)/\lambda_a$. The listed values are for $NH_3^+CD_2COO^-$. Contributions smaller than 10% are omitted. — [b] FR = Fermi resonance. — [c] Shoulder.
[d] Not used in the refinement procedure for the determination of the empirical force field.
[e] Minor components resulting from factor-group splittings.
[f] Mean value of factor-group doublet (1418.9 and 1395.5 cm^{-1}). — [g] Not investigated.

weak band (ν_5). The two antisymmetric NH_3 stretching vibrations are expected to have higher frequencies, and thus the strongest band at 3152.2 cm^{-1} could be assigned to these modes (they could not be resolved in our experiment). The ν_1/ν_2 band has a shoulder at ~3210 cm^{-1}, which is probably due to a Fermi resonance with the combination tone of the NH_3-deformation (ν_7) and CO_2-stretching (ν_8) at 1617.5 and 1596.7 cm^{-1}, respectively. The ν_3 band at 3058.2 cm^{-1} was tentatively assigned to the symmetric NH_3 stretching fundamental. The assignments for the ν_1/ν_2 and ν_3 absorptions are supported by the finding that

Table 3. Observed and calculated frequencies for $ND_3^+CH_2COO^-$, $^{15}ND_3^+CH_2COO^-$, and $ND_3^+CH_2{}^{13}COO^-$ (α-form) at 80 K.

Assignment		$ND_3^+CH_2COO^-$ ν/cm^{-1}		$^{15}ND_3^+CH_2COO^-$ ν/cm^{-1}		$ND_3^+CH_2{}^{13}COO^-$ ν/cm^{-1}		Potential energy distribution (PED)[a]
		obs.	calc.	obs.	calc.	obs.	calc.	
	ν_1	3008.0	3008.6	3008.0	3008.6	3007.7	3008.6	99 $\nu_{as}(CH_2)$
	ν_2	2972.0	2972.8	2972.8	2972.8	2972.7	2972.8	99 $\nu_s(CH_2)$
FR[b]	$2\nu_{11}$	2396.9		2388.0		2397.6		
FR[b]	$\nu_{11}+\nu_{12}$	2377.4		2370[c]		2377.9		
FR[b]	$2\nu_{12}$	2361[c]		2351.1		2362[c]		
	ν_3	overlap	2347.0	2329.4	2331.9	overlap	2347.0	90 $\nu_{as}(ND_3)$
	ν_4	2340.7	2337.3	overlap	2322.9	2340.5	2337.2	90 $\nu'_{as}(ND_3)$
	ν_5	2202.6	2202.3	2198.4[d]	2196.8	2200.2	2202.3	99 $\nu_s(ND_3)$
	ν_6	1590.0	1591.3	1587.8	1591.2	1547.1	1549.4	92 $\nu_{as}(CO_2)$, 25 $\gamma_{in}(CO_2)$
	ν_7	1439.8	1443.4	1440.0	1442.7	1437.8	1441.2	87 $\delta(CH_2)$
	ν_8	1408.5	1411.7	1407.4	1411.3	1389.4	1389.5	51 $\nu_s(CO_2)$, 25 $\nu(CC)$, 18 $\gamma_w(CH_2)$
	ν_9	1322.4	1323.1	1321.7	1323.0	1316.1	1314.6	77 $\gamma_w(CH_2)$, 19 $\nu_s(CO_2)$
	ν_{10}	1268.4	1267.1	1267.0	1265.6	1266.7	1263.3	46 $\gamma_t(CH_2)$
	ν_{11}	1192.7	1194.3	1185.1	1186.8	1192.9	1194.2	55 $\delta_s(ND_3)$, 39 $\delta'_{as}(ND_3)$, 11 $\nu(CN)$
	ν_{12}	1181.6	1183.8	1176.3	1177.9	1180.6	1183.7	85 $\delta_{as}(ND_3)$
	ν_{13}	1168.5	1160.0	1162.1	1152.8	1168.3	1160.0	60 $\delta'_{as}(ND_3)$, 33 $\delta_{as}(ND_3)$
	ν_{14}	1046.6	1047.3	1045.1	1046.3	1036.2	1047.0	37 $\gamma_r(CH_2)$, 17 $\tau(ND_3)$, 14 $\pi(ND_3)$
	ν_{15}	1004.1	1004.9	1000.8	1003.4	1003.7	1004.0	34 $\nu(CN)$, 15 $\gamma_{in}(CO_2)$, 10 $\delta(CCN)$
	ν_{16}	966.0	968.7	963.8	967.2	963.9	965.7	29 $\gamma_{in}(ND_3)$, 23 $\nu(CC)$, 22 $\delta(CCN)$, 17 $\nu_s(CO_2)$
	ν_{17}	822.8	829.8	820.2	826.5	818.0	823.8	46 $\gamma_{in}(ND_3)$, 28 $\delta(CO_2)$
	ν_{18}	771.5	777.4	770.0	775.0	768.8	771.1	54 $\pi(ND_3)$, 32 $\pi(CO_2)$, 11 $\gamma_r(CH_2)$
	ν_{19}	673.6	675.0	672.9	671.5	671.2	667.9	39 $\pi(CO_2)$, 31 $\gamma_t(CH_2)$, 22 $\nu(CN)$, 13 $\pi(ND_3)$, 13 $\gamma_{in}(CO_2)$
	ν_{20}	597.9	598.5	597.0	598.0	590.2	592.5	58 $\pi(CO_2)$, 54 $\gamma_t(CH_2)$, 48 $\gamma_{in}(CO_2)$, 13 $\delta(CCN)$, 11 $\tau(CO_2)$, 10 $\nu(CC)$
	ν_{21}	492.5	493.8	491.1	493.2	492.1	492.5	38 $\delta(CO_2)$, 33 $\gamma_{in}(CO_2)$, 20 $\delta(CCN)$, 20 $\nu(CC)$, 15 $\gamma_t(CH_2)$, 12 $\gamma_w(CH_2)$, 10 $\nu_s(CO_2)$, 10 $\delta(CH_2)$
	ν_{22}	394.7	401.5	393.0	401.3	393.7	401.4	63 $\tau(ND_3)$, 27 $\gamma_r(CH_2)$, 10 $\pi(ND_3)$
	ν_{23}	337.0	340.7	334.4	337.7	336.1	340.4	51 $\delta(CCN)$, 25 $\delta(CO_2)$, 13 $\nu(CC)$
	ν_{24}	223.2	219.1	222.6	218.6	—[e]	218.8	57 $\tau(CO_2)$, 43 $\gamma_t(CH_2)$, 24 $\gamma_r(CH_2)$, 15 $\pi(ND_3)$, 12 $\pi(CO_2)$

[a] PED is given as values of $100 \times F_s(i,i) \times L_s^2(i,a)/\lambda_a$. The listed values are for $ND_3^+CH_2COO^-$. Contributions smaller than 10% are omitted. — [b] FR = Fermi resonance. — [c] Shoulder.
[d] Mean value of factor-group doublet (2205.5 and 2191.3 cm^{-1}). — [e] Not investigated.

the ^{15}N-substitution caused expected frequency shifts of the bands in question (Figure 2c). The remaining two absorptions (ν_4 and ν_5) underwent frequency shifts in the spectra of the 2-^{13}C and ^{15}N-2-^{13}C labeled modifications (Fig. 2b and 2c), and therefore we assign the ν_4 and ν_5 bands to the antisymmetric and symmetric CH_2-stretching vibrations, respectively.

The $\nu_1-\nu_3$ NH_3 vibrational modes are expected to shift into the 2500–2100 cm^{-1} region of the spectrum upon deuterium substitution of the amino group. As can be seen from Fig. 3, the ND_3 stretching region is quite complicated, and shows a considerable amount of structure arising from Fermi resonances with overtones and combinations of fundamentals such as the ND_3 deformation. The most intense band at 2340.7 cm^{-1} could be assigned to the nearly degenerate antisymmetric ND_3 stretching vibrations, which are possibly perturbed by Fermi resonances with the overtones $2\nu_{11}$ and $2\nu_{12}$, and with the combination mode $\nu_{11}+\nu_{12}$. This assignment is compatible with the finding that the band has experienced a significant frequency shift (ca. 10 cm^{-1}) upon ^{15}N substitution (see

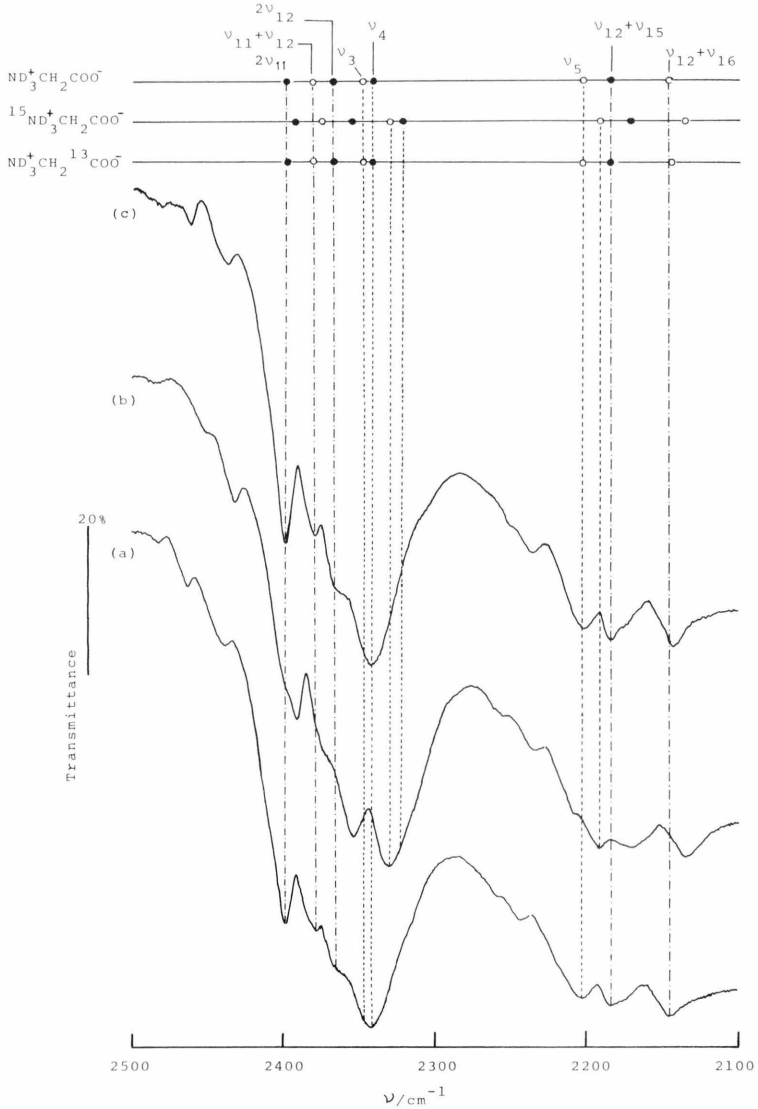

Fig.3. N−D stretching region of the IR spectra of α-$ND_3^+CH_2COO^-$ (a), α-$^{15}ND_3^+CH_2COO^-$ (b), and α-$ND_3^+CH_2{}^{13}COO$ (c) at 80 K. The final interpretation for the band assignments is indicated as symbols ν_i at the top of the spectra.

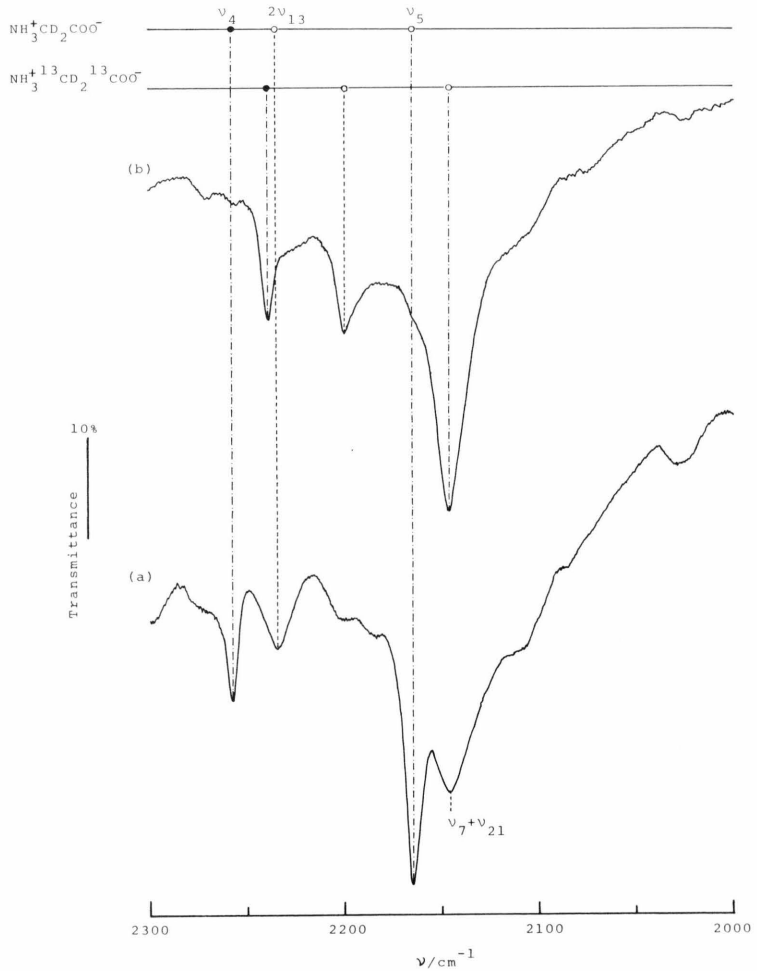

Fig. 4. Characteristic absorption bands due to C−D stretching modes of α-$NH_3^+CD_2COO^-$ (a) and α-$NH_3^+{}^{13}CD_2{}^{13}COO^-$ (b) at 80 K. The final assignments for fundamentals are indicated as symbols ν_i at the top of the spectra.

Table 4. Observed and calculated frequencies for $ND_3^+CD_2COO^-$ and $ND_3^+{}^{13}CD_2{}^{13}COO^-$ (α-form) at 80 K.

Assignment	$ND_3^+CD_2COO^-$ ν/cm^{-1}		$ND_3^+{}^{13}CD_2{}^{13}COO^-$ ν/cm^{-1}		Potential energy distribution (PED)[a]
	obs.	calc.	obs.	calc.	
FR[b] $2\nu_8$	2393.0		2395.7		
FR[b] ν_1	2349.2	2347.0	overlap	2346.8	87 $\nu_{as}(ND_3)$, 10 $\nu'_{as}(ND_3)$
ν_2	2340.3	2338.2	2339.6	2337.8	86 $\nu'_{as}(ND_3)$, 10 $\nu_{as}(ND_3)$
FR[b] ν_3	2262.9[c]	2243.4	2246.0[c]	2225.7	96 $\nu_{as}(CD_2)$
FR[b] $\nu_{10}+\nu_{12}$	2225.7		2222.8		
ν_4	overlap	2203.4	overlap	2202.9	94 $\nu_s(ND_3)$
FR[b] $\nu_{10}+\nu_{13}$	2184.7		2170[d]		
ν_5	2176.6	2175.6	2165.7	2164.0	93 $\nu_s(CD_2)$
ν_6	1580.3	1576.3	1530.0[e]	1531.8	101 $\nu_{as}(CO_2)$, 26 $\gamma_{in}(CO_2)$
ν_7	1404.6[f]	1403.7	1369.1[g]	1367.9	79 $\nu_s(CO_2)$, 30 $\nu(CC)$, 13 $\delta(CO_2)$
ν_8	1197.0	1201.1	1192.3	1198.6	39 $\delta_s(ND_3)$, 25 $\delta'_{as}(ND_3)$, 22 $\delta_{as}(ND_3)$, 17 $\nu(CN)$
ν_9	1176.5	1185.3	1177.5	1184.4	68 $\delta_{as}(ND_3)$, 16 $\delta_s(ND_3)$
ν_{10}	1168.9	1166.9	1167.0	1162.8	62 $\delta'_{as}(ND_3)$, 16 $\delta_s(ND_3)$, 16 $\nu(CN)$
ν_{11}	1134.6	1131.9	1115.7	1113.6	35 $\gamma_w(CD_2)$, 27 $\delta_s(ND_3)$, 12 $\nu(CN)$
ν_{12}	1076.7	1077.0	1065.3	1067.9	19 $\delta(CD_2)$, 13 $\pi(ND_3)$, 12 $\pi(CO_2)$
ν_{13}	1011.4	1010.2	1005.1	1004.0	55 $\delta(CD_2)$, 11 $\pi(ND_3)$
ν_{14}	957.4	955.7	947.2	943.3	33 $\gamma_{in}(ND_3)$, 28 $\delta(CCN)$, 11 $\gamma_{in}(CO_2)$
ν_{15}	921.1	909.1	906.2	902.5	24 $\delta(CO_2)$, 22 $\gamma_w(CD_2)$, 14 $\nu(CC)$
ν_{16}	872.5	865.2	865.8	858.2	34 $\pi(ND_3)$, 13 $\gamma_r(CD_2)$, 11 $\tau(ND_3)$, 11 $\pi(CO_2)$
ν_{17}	804.5	797.5	803.2	793.5	45 $\gamma_{in}(ND_3)$, 13 $\delta(CO_2)$, 11 $\gamma_w(CD_2)$
ν_{18}	710.6	714.0	706.6	706.4	44 $\pi(CO_2)$, 30 $\gamma_r(CD_2)$, 22 $\tau(ND_3)$, 13 $\pi(ND_3)$, 13 $\gamma_t(CD_2)$
ν_{19}	650.0	642.5	642.5	639.3	37 $\gamma_{in}(CO_2)$, 22 $\nu(CN)$, 11 $\pi(ND_3)$, 10 $\delta(CCN)$
ν_{20}	534.3	536.0	527.8	528.8	53 $\gamma_t(CD_2)$, 43 $\pi(CO_2)$, 20 $\nu(CC)$, 18 $\delta(CCN)$, 12 $\delta(CO_2)$, 11 $\tau(CO_2)$
ν_{21}	468.2	475.4	465.5	470.1	52 $\gamma_t(CD_2)$, 43 $\gamma_{in}(CO_2)$, 28 $\delta(CO_2)$, 18 $\pi(CO_2)$, 14 $\delta(CCN)$, 13 $\gamma_w(CD_2)$, 10 $\tau(CO_2)$, 10 $\nu(CC)$
ν_{22}	393.0	394.0	392.8	392.8	54 $\tau(ND_3)$, 33 $\gamma_r(CD_2)$, 12 $\pi(ND_3)$
ν_{23}	335.1	337.1	333.9	336.3	49 $\delta(CCN)$, 26 $\delta(CO_2)$, 13 $\nu(CC)$, 10 $\nu_s(CO_2)$
ν_{24}	222.3	213.5	—[h]	212.0	60 $\tau(CO_2)$, 43 $\gamma_t(CD_2)$, 22 $\gamma_r(CD_2)$, 14 $\pi(ND_3)$, 12 $\pi(CO_2)$

[a] PED is given as values of $100 \times F_s(i,i) \times L_s^2(i,a)/\lambda_a$. The listed values are for $ND_3^+CD_2COO^-$. Contributions smaller than 10% are omitted. — [b] FR = Fermi resonance.

[c] Not used in the refinement procedure for the determination of the empirical force field. — [d] Shoulder.

[e–g] Mean values of the respective factor-group doublets of (1544.7 and 1514.8 cm^{-1}), (1414.2 and 1394.9 cm^{-1}), and (1372.8 and 1365.3 cm^{-1}). — [h] Not investigated.

Fig. 3 b), and that the same band did practically not shift upon ^{13}C-substitution of the carboxylate group (see Fig. 3 c). On the other hand, several choices were possible for the location of the symmetric ND_3 stretching vibration, which are the three bands at 2202.6, 2184.5, and 2144.7 cm^{-1} for the N-d_3 molecule showing frequency shifts of 10.8, 15.2, and 10.3 cm^{-1}, respectively, upon ^{15}N-subsitution (see Figure 3 b). Although the normal coordinate calculations discussed later prefered the first one (2202.6 cm^{-1}), this choice has to be considered rather tentative.

The ν_4 and ν_5 bands at 3008.5 and 2972.8 cm^{-1} for the parent species underwent significant shifts to 2257.3 and 2164.5 cm^{-1}, respectively, upon deuteration of the methylene group. The CD_2-stretching region contains additional bands, as shown in Figure 4. The band at 2233.9 cm^{-1} is to be assigned to the overtone $2\nu_{13}$ in Fermi resonance with ν_4 and/or ν_5 (Fig. 4 a). A rough estimation of the intensity pattern reveals that the overtone $2\nu_{13}$ seems to borrow intensity from both the ν_4 and ν_5 modes. Furthermore, the ν_5 normal mode has a counterpart at

Table 5. Observed and calculated frequencies for $NH_3^+CH_2{}^{13}COO^-$, $NH_3^+{}^{13}CH_2COO^-$, and $NH_3^+{}^{13}CH_2{}^{13}COO^-$ (α-form) at 80 K.

Assignment		$NH_3^+CH_2{}^{13}COO^-$ ν/cm^{-1}		$NH_3^+{}^{13}CH_2COO^-$ ν/cm^{-1}		$NH_3^+{}^{13}CH_2{}^{13}COO^-$ ν/cm^{-1}	
		obs.	calc.	obs.	calc.	obs.	calc.
FR [a]	$\nu_7+\nu_8$	3190 [b]		3210 [b]		3190 [b]	
	ν_1	3157.3	3159.3	overlap	3159.2	3157.3	3159.2
	ν_2	overlap	3153.6	3153.2	3153.6	overlap	3153.6
	ν_3	3058.0	3058.3	3058.7	3058.2	3058.0	3058.2
	ν_4	3008.1	3008.6	2997.7	2996.1	2997.9	2996.1
	ν_5	2971.9	2972.7	2966.4	2965.3	2965.6	2965.3
	ν_6	1630.7	1634.0	1631.7	1634.1	1630.0	1634.0
	ν_7	1614.3	1614.2	1616.2	1615.6	1613.8	1614.2
	ν_8	1565.1	1566.1	1595.7	1596.2	1563.0	1564.7
	ν_9	1523.7	1524.5	1532.2	1532.9	1527.0	1524.3
		1493.8 [c, d]		1506.0 [c, d]		1493.0 [c, d]	
	ν_{10}	1440.3	1442.1	1442.1	1441.5	1437.3	1439.4
	ν_{11}	1397.1 [e]	1398.3	1410.9	1408.8	1389.0 [f]	1387.7
	ν_{12}	1326.7	1326.1	1329.3	1333.4	1321.5	1323.3
	ν_{13}	1314.9	1314.3	1312.6	1311.3	1310 [b]	1309.4
	ν_{14}	1138.2	1137.9	1132.8	1133.0	1131.7	1131.4
	ν_{15}	1114.1	1119.2	1114.2	1114.1	1108.7	1113.9
	ν_{16}	1036.4	1037.3	1020.3	1022.2	1020.3	1021.7
	ν_{17}	911.1	914.3	914.2	916.3	906.5	913.0
	ν_{18}	890.6	886.8	891.2	892.8	884.5	882.9
	ν_{19}	699.9	695.1	695.1	701.5	691.8	693.6
	ν_{20}	605.5	607.1	611.9	609.3	605.7	601.6
	ν_{21}	542.2	542.9	543.4	539.3	543.2	539.0
	ν_{22}	505.9	505.5	505.9	504.0	503.7	502.6
	ν_{23}	364.0	362.5	362.0	362.0	363.3	361.8
	ν_{24}	238.0	236.8	236.0	235.1	236.0	234.7

[a] FR = Fermi resonance. — [b] Shoulder. — [c] Minor components resulting from factor-group splittings.
[d] Not used in the refinement procedure for the determination of the empirical field.
[e] Mean value of factor-group doublet (1401.2 and 1393.0 cm^{-1}).
[f] Mean value of factor-group doublet (1393.5 and 1384.4 cm^{-1}).

the lower frequency side. No corresponding band was observed in the Raman spectrum of this species [26]. In addition, an analogous splitting has not been indicated in the spectrum of the 1,2-$^{13}C_2$−C-d_2 modification (see Figure 4 b). No explanation for this irregularity can be presently given.

2. $NH(D)_3$-, $CH(D)_2$-Deformation and CO_2-Stretching Region

Figure 5 presents the spectra of the parent, 1-^{13}C, and 2-^{13}C labeled species in the 1700–1200 cm^{-1} region, where a total of 8 fundamentals including three NH_3-deformational, two CO_2-stretching, and three CH_2-deformational modes should occur. Of these, the assignment of the fundamentals due to the CO_2 stretching motions was assessed straightforwardly by taking into account the ^{13}C-shifts of the vibrational modes. The intense ν_8 band at 1596.7 cm^{-1} underwent a large (ca. 32 cm^{-1}) frequency shift upon ^{13}C-substitution of the carboxylate group, whereas the same band does practically not shift upon ^{13}C-substitution of the methylene group. The intensity of the band and the result of the ^{13}C-isotopic shift strongly suggest that the ν_8 band has a considerable degree of antisymmetric CO_2-stretching character. The ν_{11} band at 1416.6 cm^{-1} has experienced large shifts by ca. 19 cm^{-1} and 6 cm^{-1} upon ^{13}C-substitution of the CO_2 and CH_2 groups, respectively, which leads us to assign this band to the symmetric CO_2-stretching mode having a substantial degree of C−C stretching character.

NH_3 bending modes form three fundamentals, one symmetric and two antisymmetric deformations, which yield infrared group frequencies around 1530 and 1620 cm^{-1}, respectively. The bands at 1633.9 (ν_6) and 1617.5 (ν_7) cm^{-1} can be reasonably assigned to

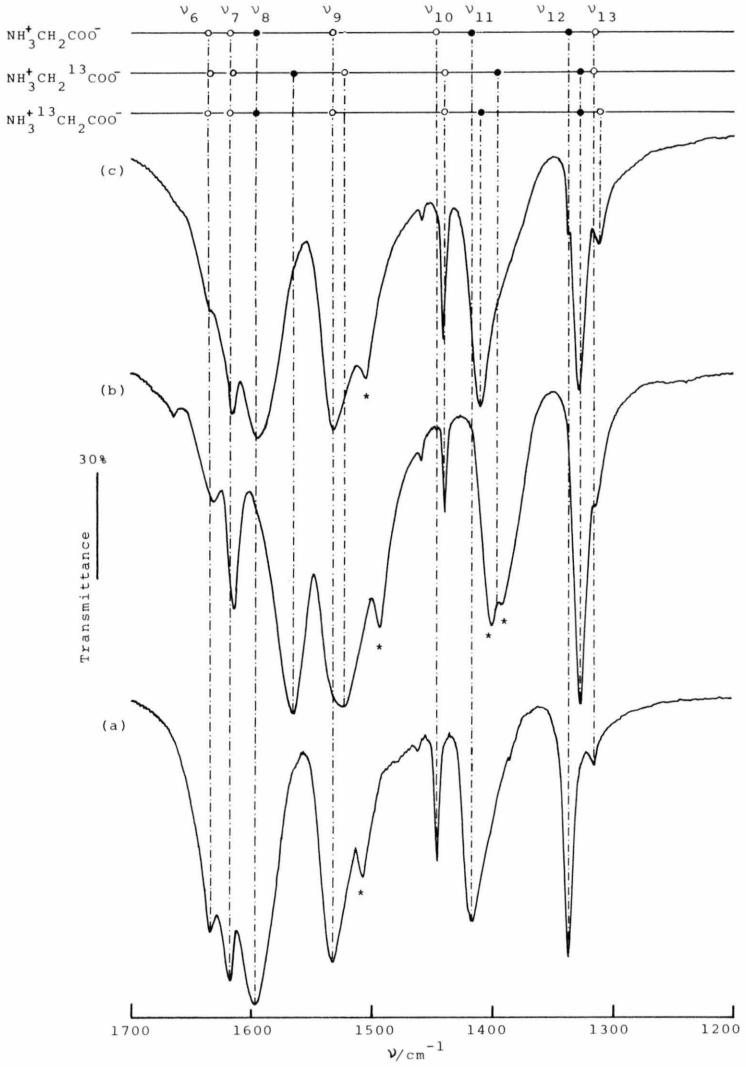

Fig. 5. Mid-infrared region of 1700–1200 cm^{-1} of the IR spectra of α-$NH_3^+CH_2COO^-$ (a), α-$NH_3^+CH_2{}^{13}COO^-$ (b), and α-$NH_3{}^{13}CH_2COO^-$ (c) at 80 K. Bands marked by an asterisk represent factorgroup splittings. Positions of fundamentals are schematically indicated by circles at the top of the spectra, together with our final assignments.

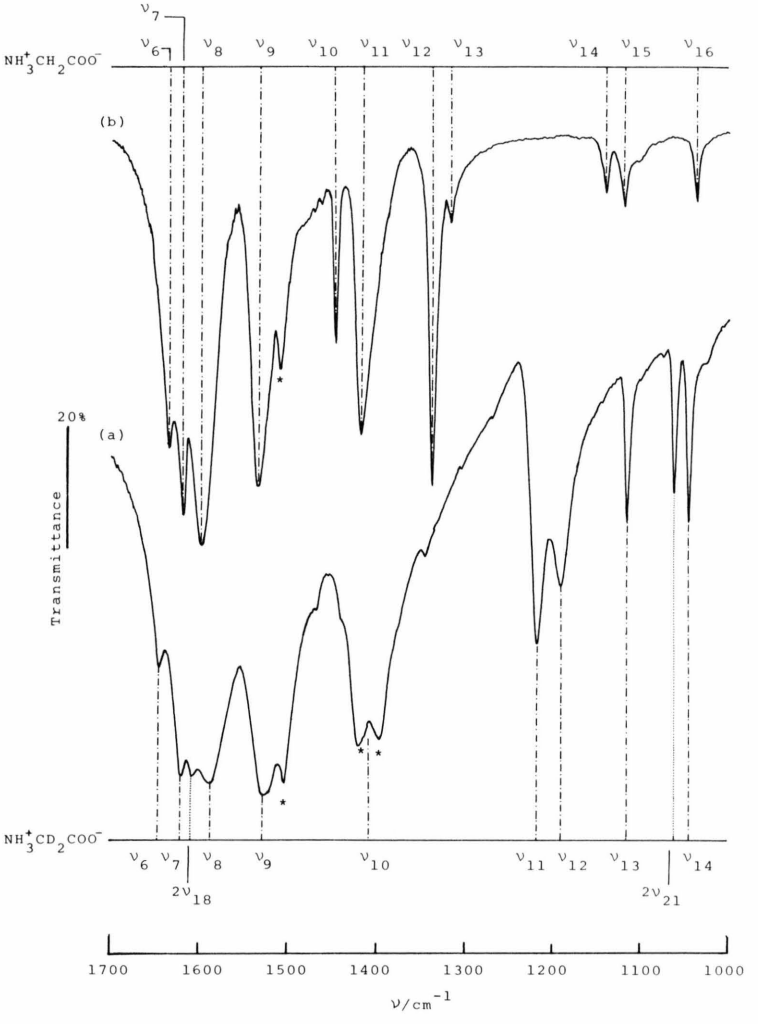

Fig. 6. Effect of C-deuteration on the IR spectrum of d_0 species; a selected region (1700–1000 cm^{-1}) of the IR spectra of α-$NH_3^+CD_2COO^-$ (a) and α-$NH_3^+CH_2COO^-$ (b) at 80 K. Bands marked by an asterisk represent factorgroup splittings. Symbols ν_i indicate the final interpretation for the band assignments.

Table 6. Observed and calculated frequencies for $^{15}NH_3^+CH_2COO^-$, $NH_3^+CH_2C^{18}O^{18}O^-$, and $^{15}NH_3^+{}^{13}CH_2COO^-$ (α-form) at 80 K.

Assignment		$^{15}NH_3^+CH_2COO^-$ ν/cm^{-1}		$NH_3^+CH_2C^{18}O^{18}O^-$ ν/cm^{-1}		$^{15}NH_3^+{}^{13}CH_2COO^-$ ν/cm^{-1}	
		obs.	calc.	obs.	calc.	obs.	calc.
FR [a]	$\nu_7+\nu_8$	3218.3		3215 [b]		3213.2	
	ν_1	3147.2	3149.0	3156.6	3159.3	3147.9	3149.0
	ν_2	overlap	3143.9	overlap	3153.6	overlap	3143.8
	ν_3	3052.0	3054.9	3058.0	3058.3	3051.9	3054.9
	ν_4	3008.5	3008.6	3008.3	3008.6	2997.7	2996.1
	ν_5	2972.9	2972.8	2972.1	2972.8	2966.4	2965.3
	ν_6	1631.4	1630.9	1632.7	1634.1	1631 [b]	1630.9
	ν_7	1616.3	1612.2	1614.7	1614.7	1615.0	1612.0
	ν_8	1594.6	1596.8	1578.3	1581.6	1593.0	1595.8
	ν_9	1528.3	1527.6	1528.9	1529.5	1525.0	1527.4
		1502.0 [c, d]		1500.3 [c, d]		1503.4 [c, d]	
	ν_{10}	1445.1	1443.3	1442.0	1442.3	1441.5	1440.9
	ν_{11}	1418.1	1418.0	1402.7	1403.3	1411.1	1408.0
	ν_{12}	1335.4	1333.9	1323.1	1324.7	1327.7	1331.6
	ν_{13}	1310.8	1316.0	1310 [b, d]	1314.0	1308.3	1309.6
	ν_{14}	1134.8	1135.4	1137.7	1138.2	1128.8	1129.3
	ν_{15}	1117.4	1116.7	1119.1	1117.3	1112.3	1111.0
	ν_{16}	1027.0	1031.4	1033.8	1026.9	1009.7	1015.6
	ν_{17}	917.6	917.0	915.9	910.5	914.0	915.7
	ν_{18}	895.9	895.6	872.6	872.9	889.6	892.2
	ν_{19}	703.0	697.6	686.8	690.9	695.1	696.3
	ν_{20}	612.6	614.9	607.4	608.9	611.2	609.1
	ν_{21}	543.9	543.1	541.5	540.5	543.8	539.1
	ν_{22}	503.9	505.8	496.1	495.4	501.8	502.9
	ν_{23}	359.7	358.4	355.4	353.5	359.3	357.7
	ν_{24}	235.5	236.0	230.2	232.4	235.2	233.9

[a] FR = Fermi resonance. — [b] Shoulder. — [c] Minor components resulting from factor-group splittings.
[d] Not used in the refinement procedure for the determination of the empirical force field.

the two antisymmetric NH_3 deformational modes. On the other hand, the ν_9 band at 1532.6 cm^{-1} is assignable to the symmetric NH_3 deformational mode. However, the same band shifts by ca. 9 cm^{-1} upon ^{13}C-substitution of the carboxylate group, which suggests that the ν_9 band may have an appreciable contribution from antisymmetric CO_2-stretching. The ν_9 band has an additional minor component at a lower frequency at about 1530 cm^{-1}. This splitting is presumably due to the site-splitting resulting from different crystal sites of glycine. The interpretation is supported by an often similar structure of the corresponding bands in the spectra of other isotopic species.

The remaining three bands at 1445.9 (ν_{10}), 1336.8 (ν_{12}), and 1315.3 (ν_{13}) cm^{-1} can be related to the CH_2 vibrational motions, since these bands have disappeared in the spectrum of C-deuterated glycine, as shown in Figure 6a. The 1445.9 cm^{-1} band (ν_{10}), which is reasonably assigned to the CH_2-scissoring mode, shifts into the 1100–1000 cm^{-1} region of the spectrum of the C-d_2 species, and exhibits a doublet structure with components centered at 1060.3 cm^{-1} and 1044.2 cm^{-1} (Figure 6a). We tentatively assign the latter band to the CD_2-scissoring vibration. The origin of the former band absorption is not well understood. One explanation for this band is that it arises from the overtone $2\nu_{21}$ (= 1059.2 cm^{-1}) standing in Fermi resonance with the CD_2-scissoring mode.

The 1336.8 (ν_{12}) and 1315.3 (ν_{13}) cm^{-1} bands, conventionally regarded as pure CH_2-wagging and CH_2-twisting vibrations, respectively, seem to have contributions from several group modes in view of the following findings:

i) The pattern of the ^{13}C-isotopic shifts observed for the ν_{12} band was similar to that seen for the ν_{11} band (approx. CO_2-symmetric stretch + C–C stretching), suggesting a strong coupling between these bands (cf. Figure 5).

ii) Deuteration of the amino group shifts these 1336.8 (ν_{12}) and 1315.3 (ν_{13}) cm^{-1} bands down to

1322.4 (ν_9) and 1268.4 (ν_{10}) cm^{-1} with a marked change in their relative intensities, as indicated in Figure 7.

This later observation demonstrates that group coordinate compositions in the ν_{12} and ν_{13} modes can change strongly in response to the N-deuterion.

The three NH_3-deformational modes (ν_6, ν_7, and ν_9) are expected to shift into the 1200 cm^{-1} region of the spectrum of the N-d_3 species, and thus the strong bands at 1192.7 (ν_{11}), 1181.6 (ν_{12}), and 1168.5 (ν_{13}) cm^{-1} seen in Fig. 7a can be related to these vibrational modes. By taking into account their relative intensities, the band at the highest frequency is assigned to the symmetric ND_3-deformational mode, and the others to the antisymmetric ND_3-deformational modes.

3. Far-Infrared Region

Representative spectra (550–100 cm^{-1}) of the parent, ^{18}O-, C- and N-deuterated species at 80 K are shown in Fig. 8, where the 394.7 cm^{-1} band in the spectrum of the N-d_3 species could not be detected in the corresponding room temperature spectrum. In this spectral region, four fundamentals due to NH_3- and CO_2-torsional, CO_2-rocking, and CCN-skeletal modes should occur. The ν_{21} modes at 544.7 cm^{-1} for the parent species is sensitive to both the C- and N-deuteration, shifting to 529.6 and 394.7 cm^{-1} in the spectra of the C-d_2 and the N-d_3 species, respectively (see Fig. 8c and d). Based upon this observation, we assign the 544.7 cm^{-1} band to the NH_3-torsional mode having a substantial degree of CH_2-rocking character. The ν_{22} band at 506.9 cm^{-1} underwent a large frequency shift by 10 cm^{-1} upon ^{18}O-substitution of the CO_2 group, leading us to assign conveniently this band to a CO_2-rocking mode. However, the same band also underwent frequency shifts of 34.5 and 14.4 cm^{-1} upon C- and N-deuteration, respectively, which suggests that this mode is highly mixed combination of local vibrational modes associated with the amino and methylene groups. The ν_{23} band at 364.3 cm^{-1}, previously assigned to a CCN bending vibration, seems to correspond to an intimate mixture of several group vibrations, as demonstrated by the 27.3 cm^{-1} ND_3-induced shift as well as the 10 cm^{-1} shift upon ^{18}O-subsitution of the CO group. The assignment of the remaining CO_2-torsional mode is based upon the arguments given by Machida et al. [18–19], and thus the absorptions at 238.4 and 217.2 cm^{-1} are considered to have dominant contributions from the CO_2-torsional mode, whereas the absorption below 200 cm^{-1} might be considered as lattice vibrations. Support for this assignment comes from the 8.2 cm^{-1} shift of the 238.4 cm^{-1} band and the 6.0 cm^{-1} shift of the 217.2 cm^{-1} band in the spectrum of the ^{18}O-labeled species (see Figure 8 b).

In oder to resolve the ambiguous part of the assignment described in this section and to obtain a more reliable description of the normal modes in terms of group modes, a normal coordinate analysis was carried out, see next section.

B. Normal Coordinate Analysis

A normal coordinate analysis (NCA) was carried out based upon Wilson's GF-matrix formulation [27]. Our computer programs allowed us to calculate Wilson's G-matrix elements, the solution of secular equations, and the best values of force constants through an iterative procedure. Details of the numerical calculations are given below.

1. Structure and Internal Coordinates

The **G**-matrix was calculated by using the structural data obtained by the precise neutron diffraction study on α-glycine [21]. Figure 9 represents a schematic structural view of the α-glycine molecule. Of particular important is the fact that the atoms O_4, O_5, and H_8 deviate significantly from the $C_1-C_2-N_3$ plane, and thus the α-glycine molecule has no symmetry element. The geometrical parameters of α-glycine employed in this calculation are listed in Table 7, where the symbols and numbering of the atoms are in accord with the notations given in Fig. 9, and the notation t indicates the torsional angles of the skeletal atoms. Figure 9 also gives the definition of stretching and bending internal coordinates used in this work. On the assumption that the atoms C_2, C_1, O_4, and O_5 are coplanar, two CO_2-rocking coordinates, which are in-plane and out-of-plane with respect to the $C-CO_2$ plane, are introduced:

i) the in-plane CO_2-rocking coordinate (γ) defined as the angle between the C_1-C_2 bond and the line bisecting the angle θ, i.e. $\gamma=(1/2)(\phi-\psi)$;

ii) the out-of-plane CO_2-rocking coordinate (π) defined as the angle between the C_1-C_2 bond and the $O-C-O$ plane.

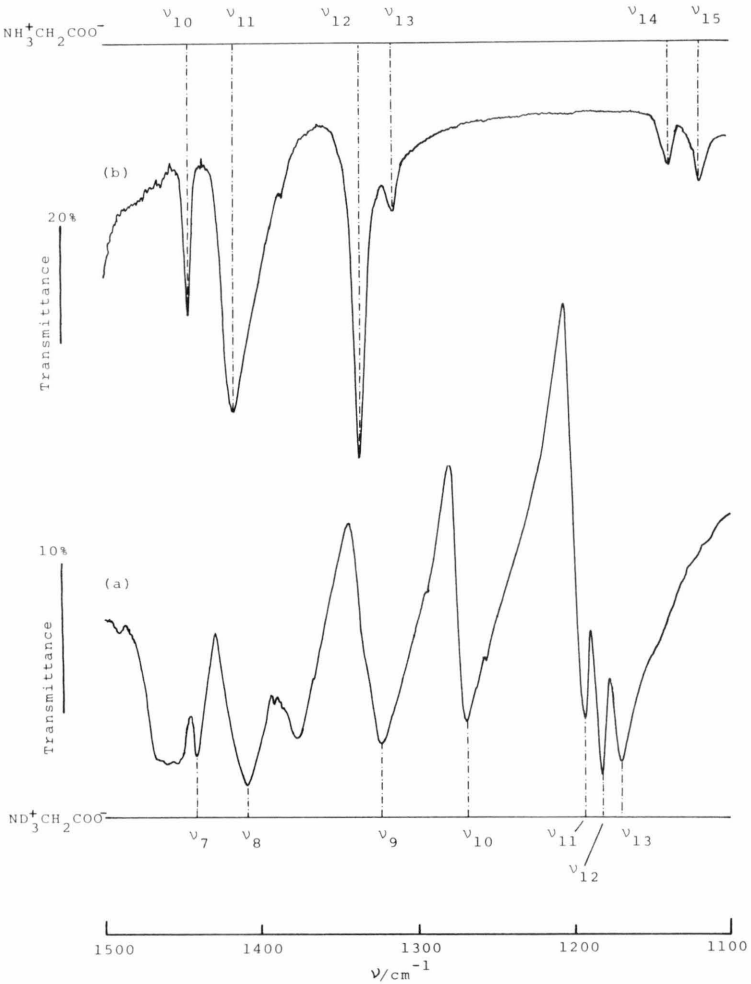

Fig. 7. Effect of N-deuteration on the IR spectrum of d_0 species; the 1500–1100 cm^{-1} region of the IR spectra of α-ND$_3^+$CH$_2$COO$^-$ (a) and α-NH$_3^+$CH$_2$COO$^-$ (b) at 80 K. The final assignments for fundamentals are indicated as symbols ν_i.

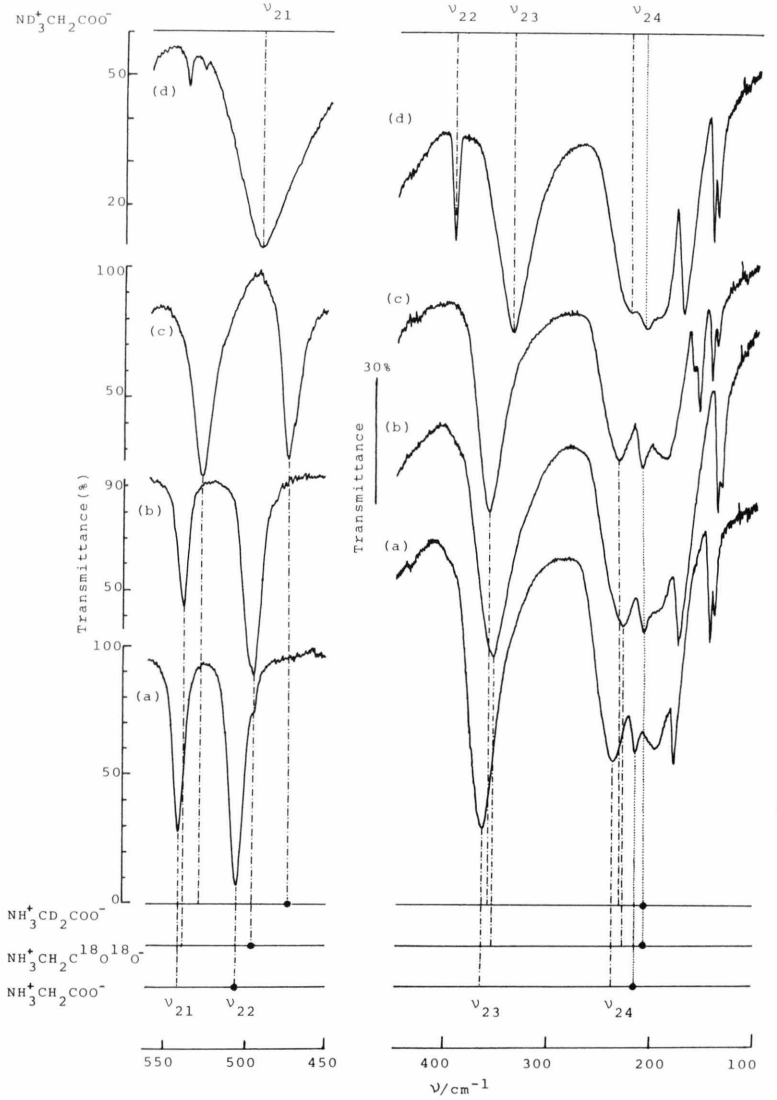

Fig. 8. Far-infrared region of 550–100 cm^{-1} of the IR spectra of α-NH$_3^+$CH$_2$COO$^-$ (a), α-NH$_3^+$CH$_2$C^{18}O^{18}O$^-$ (b), α-NH$_3^+$CD$_2$COO$^-$ (c), and α-ND$_3^+$CH$_2$COO$^-$ (d) at 80 K. Bands appearing below 200 cm^{-1} are considered to be lattice modes. The final interpretation for the band assignments is indicated as symbols ν_i.

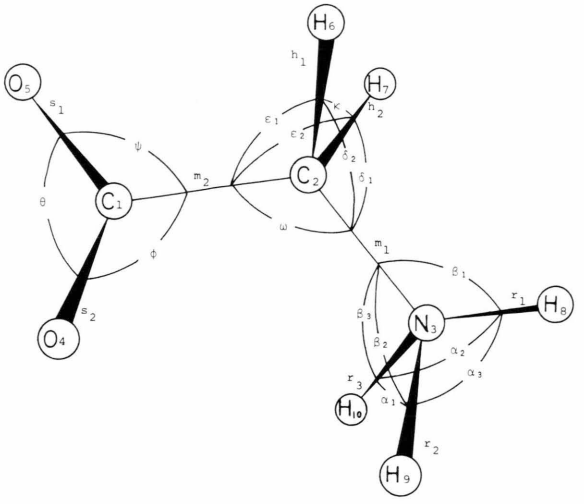

Fig. 9. Definition of internal coordinates for α-glycine. The internal coordinates for CO_2 in-plane and out-of-plane rocking and torsion of NH_3 and CO_2 groups are defined in the text.

In the equilibrium state of α-glycine, the angle π is 0° to a very good approximation [21, 22].

The torsional coordinates associated with the CO_2 and NH_3 groups are chosen as linear combinations of all possible four mass-torsional coordinates as follows:

$$\tau_1(CO_2)=\tfrac{1}{6}(\tau_{4123}+\tau_{4126}+\tau_{4127}+\tau_{5123}+\tau_{5126}+\tau_{5127}),$$

$$\tau_2(NH_3)=\tfrac{1}{9}(\tau_{8321}+\tau_{8326}+\tau_{8327}+\tau_{9321}+\tau_{9326}+\tau_{9327}+\tau_{\underline{10}321}+\tau_{\underline{10}326}+\tau_{\underline{10}327}),$$

where the subscripts correspond to the numbering of the atoms given in Figure 9. In spite of the general asymmetry of the glycine molecule, we introduce several local-symmetry coordinates as given in Table 8. In order to remove two redundant coordinates involved within the bending internal coordinates associated with the NH_3- and $-CH_2$-groups, appropriate linear combinations of these internal coordinates are required. In constructing the nonredundant set of local-symmetry coordinates, the distorted tetrahedral configuration around the amino and methylene groups was taken into consideration, as demonstrated by the correction (non-unity) coefficients introduced into these local-symmetry coordinates (see Table 8). Generally accepted local-symmetry coordinates involving the N–H, C–H, and C–O stretching internal coordinates were also introduced in order to make it easier to compare our work with previous studies on glycine.

Table 7. Structural parameters for α-glycine[a].

Notation[b]	Value	Notation[b]	Value
$r_1(N_3-H_8)$	0.1054 nm	$\varkappa(H_6C_2H_7)$	108.02°
$r_2(N_3-H_9)$	0.1037 nm	$\delta_1(N_3C_2H_7)$	109.05°
$r_3(N_3-H_{10})$	0.1025 nm	$\delta_2(N_3C_2H_6)$	108.51°
$h_1(C_2-H_6)$	0.1090 nm	$\omega(C_1C_2N_3)$	111.85°
$h_2(C_2-H_7)$	0.1089 nm	$\varepsilon_1(C_1C_2H_6)$	108.81°
$m_1(C_2-N_3)$	0.1476 nm	$\varepsilon_2(C_1C_2H_7)$	110.50°
$m_2(C_1-C_2)$	0.1526 nm	$\theta(O_4C_1O_5)$	125.45°
$s_1(C_1-O_4)$	0.1250 nm	$\phi(C_2C_1O_4)$	117.46°
$s_2(C_1-O_5)$	0.1251 nm	$\psi(C_2C_1O_5)$	117.09°
$\alpha_1(H_9N_3H_{10})$	106.66°	$t(s_1)$[c]	18.9°
$\alpha_2(H_8N_3H_{10})$	107.03°	$t(s_2)$[c]	198.2°
$\alpha_3(H_8N_3H_9)$	108.71°	$t(h_1)$[d]	119.9°
$\beta_1(C_2N_3H_8)$	112.09°	$t(h_2)$[d]	238.3°
$\beta_2(C_2N_3H_9)$	111.73°	$t(r_1)$[e]	182.7°
$\beta_3(C_2N_3H_{10})$	110.37°	$t(r_2)$[e]	60.4°
		$t(r_3)$[e]	302.0°

[a] Geometry at equilibrium according to [21].
[b] Symbols are in accord with the notations given in Figure 9.
[c] The clockwise torsion angle between the $N_3C_2C_1$ plane and the $C_2C_1O_{4(5)}$ plane.
[d] The clockwise torsion angle between the $N_3C_2C_1$ plane and the $H_{6(7)}C_2C_1$ plane.
[e] The clockwise torsion angle between the $N_3C_2C_1$ plane and the $H_{8(9,10)}N_3C_2$ plane.

2. Constraints to the General Valence Force Field and NCA Results

The overall potential function of glycine crystal is quite complicated owing to the presence of a large number of intra- and intermolecular terms. Because of the lack of frequency data below 100 cm^{-1}, we were forced to remove the intermolecular terms from the mathematical expression of the potential function. Therefore, note that the force field derived from the observed frequencies is not free from intermolecular interactions amongst glycine molecules.

Since the glycine molecule has no overall symmetry, its intramolecular general valence force field involves 300 parameters. Our experimentally determined frequency data were not sufficient to determine the 300 force constants, and thus a number of constraints were imposed on the force field. The scheme of constraints used for the present molecule is very similar to that proposed by Hollenstein and Günthard [6, 29]. The following criteria are shomewhat specific for the glycine molecule:

i) Since the NH_3 torsional motion would practically not be separated from its neighboring higher frequency modes, the interaction constants of $\Delta\tau_2$ with $\Delta\pi$ and $\pi(NH_3)$ are taken into consideration.

ii) A redundant set of force constants associated with the NH_3-group was introduced according to the convention used by Hollenstein and Günthard [28]. On the other hand, an independent set of force constants refering to the local-symmetry coordinates of the CH_2-scissoring (S_s), -wagging (S_w), -twisting (S_t), -rocking (S_r), and CCN-bending (S_b) motion was chosen. In introducing potential constants associated with these local-symmetry coordinates, exceptions are the interaction constants of $\Delta\theta$ with ΔS_s and ΔS_w, which were not taken into consideration in the case of propionate ion [5].

iii) Several local-symnmetry approximations were employed:

a) C_{2v} for $-CO_2$,

b) C_{3v} for $-NH_3$,

c) C_s for NH_3-CH_2-C, i.e. interaction constants between quasi-A' symmetric and -A'' antisymmetric coordinates with respect to the pseudo molecular symmetry (C−C−N) plane are omitted (cf. Figure 9). In addition, interaction force constants of $\Delta\theta$ and of $\Delta\gamma$ with the quasi-A'' coordinates except for $\gamma_t(CH_2)$ are omitted.

iv) Within the $N-CH_2-C$ fragment, interaction force constants of Δm_1 were assumed to be equal to the corresponding constants of Δm_2.

The application of these assumptions left 50 force constants, 17 of which being diagonal force constants. A choice of initial values of the force constants was carried out both by comparison with structurally related molecules [5, 25, 29] and by reference to earlier investigations [13, 18]. These force constants were refined simultaneously to fit a total of 307 experimentally determined frequencies by least-squares iterative procedure. The observed frequency data are distributed amongst 14 isotopic analogs of the glycine molecule, and the individual frequency choice made for each isotopic molecule can be extracted by inspection of Tables 1–6. The final set of refined force constants assocciated with the internal coordinates are given in Table 9. This strictly empirical potential function reproduces the experimental frequencies with a root-mean-squares (rms) deviation of 3.32 cm^{-1}. The normal vibrational frequencies of the parent and its deuterated derivatives calculated from the empirical force field are listed in Tables 1–4, together with an approximate description of the normal modes in terms of the potential energy distribution (PED). The calculated frequencies for the ^{13}C, ^{15}N, and ^{18}O isotopic species are collected in Tables 5 and 6.

Table 8. Local symmetry coordinates for α-glycine.

Symmetry coordinate	Notation	Description
$(1/\sqrt{6})(2\Delta r_1 - \Delta r_2 - \Delta r_3)$	$\nu_{as}(NH_3)$	antisym NH_3 str
$(1/\sqrt{2})(\Delta r_2 - \Delta r_3)$	$\nu'_{as}(NH_3)$	
$(1/\sqrt{3})(\Delta r_1 + \Delta r_2 + \Delta r_3)$	$\nu_s(NH_3)$	sym NH_3 str
$(1/\sqrt{2})(\Delta h_1 - \Delta h_2)$	$\nu_{as}(CH_2)$	antisym CH_2 str
$(1/\sqrt{2})(\Delta h_1 + \Delta h_2)$	$\nu_s(CH_2)$	sym CH_2 str
$(1/\sqrt{2})(\Delta s_1 - \Delta s_2)$	$\nu_{as}(CO_2)$	antisym CO_2 str
$(1/\sqrt{2})(\Delta s_1 + \Delta s_2)$	$\nu_s(CO_2)$	sym CO_2 str
Δm_1	ν(CN)	CN str
Δm_2	ν(CC)	CC str
$(1/\sqrt{6})(2a\,\Delta\alpha_1 - b\,\Delta\alpha_2 - c\,\Delta\alpha_3)$ [a]	$\delta_{as}(NH_3)$	antisym NH_3
$(1/\sqrt{2})(b\,\Delta\alpha_2 - c\,\Delta\alpha_3)$ [a]	$\delta'_{as}(NH_3)$	deform
$(1/\sqrt{6})(a\,\Delta\alpha_1 + b\,\Delta\alpha_2 + c\,\Delta\alpha_3 - d\,\Delta\beta_1 - e\,\Delta\beta_2 - f\,\Delta\beta_3)$ [a]	$\delta_s(NH_3)$	sym NH_3 deform
$(1/\sqrt{6})(2d\,\Delta\beta_1 - e\,\Delta\beta_2 - f\,\Delta\beta_3)$ [a]	$\gamma_{in}(NH_3)$	in-plane NH_3 rock
$(1/\sqrt{2})(e\,\Delta\beta_2 - f\,\Delta\beta_3)$ [a]	$\pi(NH_3)$	out-of-plane NH_3 rock
$(1/\sqrt{6})(a\,\Delta\alpha_1 + b\,\Delta\alpha_2 + c\,\Delta\alpha_3 + d\,\Delta\beta_1 + e\,\Delta\beta_2 + f\,\Delta\beta_3)$ [a]		redundant
$(1/\sqrt{20})(4t\,\Delta\varkappa - u\,\Delta\delta_1 - v\,\Delta\delta_2 - x\,\Delta\varepsilon_1 - y\,\Delta\delta_2)$ [b]	$\delta(CH_2)$	CH_2 sciss
$(1/2)(u\,\Delta\delta_1 + v\,\Delta\delta_2 - x\,\Delta\varepsilon_1 - y\,\Delta\varepsilon_2)$ [b]	$\gamma_w(CH_2)$	CH_2 wag
$(1/\sqrt{30})(-t\,\Delta\varkappa - u\,\Delta\delta_1 - v\,\Delta\delta_2 + 5w\,\Delta\omega - x\,\Delta\varepsilon_1 - y\,\Delta\varepsilon_2)$ [b]	δ(CCN)	CCN bend
$(1/2)(-u\,\Delta\delta_1 + v\,\Delta\delta_2 - x\,\Delta\varepsilon_1 + y\Delta\varepsilon_2)$ [b]	$\gamma_t(CH_2)$	CH_2 twist
$(1/2)(-u\,\Delta\delta_1 + v\,\Delta\delta_2 + x\,\Delta\varepsilon_1 - y\,\Delta\varepsilon_2)$ [b]	$\gamma_r(CH_2)$	CH_2 rock
$(1/\sqrt{6})(t\,\Delta\varkappa + u\,\Delta\delta_1 + v\,\Delta\delta_2 + w\,\Delta\omega + x\,\Delta\varepsilon_1 + y\,\Delta\varepsilon_2)$ [b]		redundant
$\Delta\gamma$	$\gamma_{in}(CO_2)$	in-plane CO_2 rock
$\Delta\theta$	$\delta(CO_2)$	OCO bend
$\Delta\pi$	$\pi(CO_2)$	out-of-plane CO_2 rock
$\Delta\tau_1$	$\tau(CO_2)$	CO_2 torsion
$\Delta\tau_2$	$\tau(NH_3)$	NH_3 torsion

[a] Correction coefficients for the distorted tetrahedral configuration around the NH_3 group: $a=0.9508594$, $b=0.9578177$, $c=0.9888713$, $d=1.0484304$, $e=1.0413971$, and $f=1.0083990$.

[b] Correction coefficients for the distorted tetrahedral configuration around the CH_2 group: $t=0.9612078$, $u=1.006935$, $v=0.9807512$, $w=1.0323114$, $x=0.9989827$, and $y=1.0181608$.

Table 9. Empirical force constants for α-glycine [a].

Notation [b]	Values	Notation	Values
		Stretch	
10^7 K_r/N nm^{-1}	5.3821 ± 0.0032	10^7 K_{m_1}/N nm^{-1}	4.2613 ± 0.1307
10^7 K_h/N nm^{-1}	4.8764 ± 0.0038	10^7 K_{m_2}/N nm^{-1}	3.5582 ± 0.2359
10^7 K_s/N nm^{-1}	9.3003 ± 0.2581		
		Bend	
10^9 H'_α/N nm	0.7160 ± 0.0023	10^9 H_{Sr}/N nm	0.6063 ± 0.0157
10^9 H'_β/N nm	0.5525 ± 0.0094	10^9 H_γ/N nm	5.5312 ± 0.1690
10^9 H_{Ss}/N nm	0.5968 ± 0.0034	10^9 H_θ/N nm	1.7345 ± 0.0889
10^9 H_{Sw}/N nm	0.6906 ± 0.0076	10^9 H_π/N nm	0.7867 ± 0.0126
10^9 H_{Sb}/N nm	2.3187 ± 0.1031	10^9 H_{τ_1}/N nm	0.6650 ± 0.0330
10^9 H_{St}/N nm	0.5458 ± 0.0059	10 H_{τ_2}/N nm	0.6793 ± 0.0131
		Stretch-stretch interaction	
10^7 k_r/N nm^{-1}	0.0013 ± 0.0023	10^7 k_m/N nm^{-1}	−0.0205 ± 0.1360
10^7 k_h/N nm^{-1}	0.0577 ± 0.0038	10^7 k_{m_2s} N nm^{-1}	−0.4371 ± 0.1037
10^7 k_s/N nm^{-1}	1.4680 ± 0.2581		
		Stretch-bend interaction	
10^8 $f_{s\theta}$/N	1.3089 ± 0.1234	10^8 f_{mSw}/N	0.1814 ± 0.0225
10^8 $f_{s\gamma}$/N	−1.1454 ± 0.1358	10^8 f_{mSb}/N	0.3566 ± 0.0654
10^8 $f'_{m_1\alpha}$/N	−0.3126 ± 0.0149	10^8 $f_{m_2\theta}$/N	−0.0237 ± 0.0730
10^8 f_{mSs}/N	−0.0426 ± 0.0380		
		Bend-bend interaction	
10^9 h'_β/N nm	−0.1051 ± 0.0094	10^9 h_{SsSw}/N nm	−0.0104 ± 0.0047
10^9 $h'_{\alpha\beta}$/N nm	−0.1142 ± 0.0071	10^9 h_{SwSb}/N nm	0.3140 ± 0.0443
10^9 $h_{\beta_1 Ssw}$/N nm	−0.0258 ± 0.0132	10^9 $h_{\beta_2 Str}$/N nm	−0.0952 ± 0.0026
10^9 $h_{\beta_2 Ssw}$/N nm	0.0229 ± 0.0094	10^9 $h_{\pi St}$/N nm	0.3761 ± 0.0055
10^9 $h_{\beta_1 Sb}$/N nm	0.1124 ± 0.0279	10^9 $h_{\pi Sr}$/N nm	−0.1590 ± 0.0155
10^9 $h_{\beta_2 Sb}$/N nm	0.1212 ± 0.0212	10^9 $h_{\gamma St}$/N nm	−0.4112 ± 0.0219
10^9 $h_{\gamma Sb}$/N nm	1.2602 ± 0.0917	10^9 $h_{\theta St}$/N nm	−0.1559 ± 0.0109
10^9 $h_{\gamma Ssw}$/N nm	0.7376 ± 0.0509	10^9 h_{StSr}/N nm	−0.0905 ± 0.0110
10^9 $h_{\theta Ss}$/N nm	0.0729 ± 0.0329	10^9 $h_{\beta_2\tau_2}$/N nm	−0.0351 ± 0.0064
10^9 $h_{\theta Sw}$/N nm	−0.0233 ± 0.0163	10^9 $h_{\pi\tau_2}$/N nm	−0.0521 ± 0.0097
10^9 h_{SsSb}/N nm	0.4102 ± 0.0337		

[a] The errors shown are standard deviations. — [b] Primed quantities follows the convention given in [28].

3. Discussion

This section brings a brief discussion in reference to assignments and the constrained force field.

a) Additional Comments on Vibrational Assignments

The reporduction of the 307 input data is satisfactory (rms deviation 3.32 cm^{-1}), with only few exceptions. Several relatively large differences between calculated and observed values occur especially for the NH(D) and CH(D) stretching frequencies, which may be attributed to appreciable anharmonicity in these vibrational modes. For the C-d_2 species (Table 2), the respective observed frequencies of 1643.7 and 1619.6 cm^{-1} for ν_6 and ν_7 are slightly high in comparison with the corresponding frequencies of 1633.9 and 1617.5 cm^{-1} for the parent species (Table 1). These frequencies are probably forced up by Fermi resonance with the overtone $2\nu_{18} = 1606$ cm^{-1}. Such modes involved in strong Fermi resonance were not included in the frequency data base.

The following particular aspects concerning the relation between normal coordinates and local-symmetry coordinates are worth while to mention.

i) The higher frequency vibrations above 1600 cm^{-1} appear to be reasonably pure in character. However, as demonstrated by PED descriptions for several $NH(D)_3$-stretching and -deformational frequencies, strong mixing is pronounced between quasi-A' symmetric and -A'' antisymmetric coordinates: e.g. α) the ν_6 normal mode for the parent species corresponds to a complicated vibration containing PED contributions of 48% from the quasi-A'' $\delta'_{as}(NH_3)$ and 45% from the quasi-A' $\delta_{as}(NH_3)$ (cf. Table 1), β) the ν_2 normal mode for the d_5 species has a substantial degree of the quasi-A'' $\nu'_{as}(ND_3)$ character, but the same mode contains a PED-contribution of 10% from the quasi-A' $\nu_{as}(ND_3)$ coordinate (see Table 4).

The appreciable departure of the structural parameters for the NH_3-CH_2-portion from a local C_s-symmetry is reflected in a large number of G-matrix cross-terms between quasi-A' and -A'' local-symmetry coordinates. This can result in a considerable amount of mixing between quasi-A' and -A'' coordinates in spite of the introduction of the C_s local-symmetry constraint to the potential constants associated with the NH_3-CH_2-moiety (cf. constraint iii) in the preceding section).

ii) Almost all normal modes bellow 1600 cm^{-1} are extensively intermixed group modes, as can be seen from the PED given in Tables 1–4; the compositions varying strongly from species to species. The following is of particular interest:

α) In $NH_3^+CH_2COO^-$, the methylene scissoring vibration, $\delta(CH_2)$, is involved essentially in one fundamental, ν_{10}, whereas the quasi-A' methylene wagging mode, $\gamma_w(CH_2)$, makes the respective PED contributions of 20, 18, 57 and 12% to the ν_{11}, ν_{12}, ν_{13}, and ν_{22} normal modes, furthermore strongly mixed with the quasi-A'' CH_2 twisting mode, $\gamma_t(CH_2)$, except for ν_{11} (see Table 1). The PED in the ν_{12} and ν_{13} normal modes at 1336.8 and 1315.3 cm^{-1} would require a revision of the traditional descriptions for these absorptions as the methylene-wagging and -twisting vibrations, respectively. The corresponding normal modes in $ND_3^+CH_2COO^-$ might be located in the 1322.4 (ν_9) and 1268.4 (ν_{10}) cm^{-1} bands, respectively. However, the composition of group coordinates was found to change strongly from the parent to the N-d_3 species (compare ν_{12}/ν_{13} in Table 1 with ν_9/ν_{10} in Table 3). This change of mixing is reflected in a marked difference in the band contour between the ν_{12}/ν_{13} bands of the d_0 species and the ν_9/ν_{10} bands of the N-d_3 species (cf. Fig. 7).

β) The PED in $NH_3^+CH_2COO^-$ indicates extensive dispersion of the fingerprint CO_2-deformational ($\delta(CO_2)$) and in-plane CO_2-rocking ($\gamma_{in}(CO_2)$) coordinates, making it difficult to specify any one band to these motions. The latter coordinate seems to couple intimately with the CH_2-twisting vibration ($\gamma_t(CH_2)$), as demonstrated by the PED of ν_{19}, ν_{20}, ν_{22}, and ν_{24} (see Table 1). Such coupling is also noticed for ν_{19}, ν_{21}, and ν_{22} in $NH_3^+CD_2COO^-$, for $\nu_{19}-\nu_{21}$ in $ND_3^+CH_2COO^-$, and for ν_{21} in $ND_3^+CD_2COO^-$ (see Tables 2–4).

γ) The PED in $NH_3^+CH_2COO^-$ shows the skeletal C–C stretching coordinate (ν(CC)) to be evenly distributed among the ν_{11}, ν_{18}, ν_{20}, and ν_{23} bands, and it is difficult to specify one band as the ν(CC) mode, although the ν_{18} band at 897.2 cm^{-1} may be considered as characteristic for this motion. Similarly, the skeletal C–N stretching coordinate (ν(CN)) is spread over a number of frequencies in the d_0, C-d_2, N-d_3, and d_5 species, but a substantially higher PED contribution of 54% from ν(CN) should be noted for the ν_{16} band at 1036.9 cm^{-1} in the d_0 species (see Table 1).

b) Empirical Valence Force Field

The potential function employed in this study does not include intermolecular interaction terms such as due to the hydrogen bonding network in the glycine crystal. Therefore the present potential function should be considered to be strictly empirical. However, our empirical force field is of practical value in view of the transferability of force constants to more complicated molecules. The following views are worthy of a brief discussion (see Table 9).

i) A statistically well-defined set of force constants has been found through the least-squares refinement computation with only few exceptions. Among the interaction force constants, k_r, k_m, and $f_{m_2\theta}$ turned out to be indeterminable from our experimental data; i.e. the magnitude of these force constants was smaller than their statistical dispersion, that is they are not significantly different from zero.

ii) An inspection of the values given in Table 9 reveals that most of the interaction force constants are evidently different from zero. The inclusion of the characteristic frequencies from the ^{13}C-, ^{15}N-, and

^{18}O-labeled species is essential for the determination of the empirical force field and might increase the precision of important force constants associated with the heavy atom skeleton. A number of previously uncertain or undetermined parameters, most notably force constants relating to the $C-C\begin{smallmatrix}O\\O\end{smallmatrix}$ fragment, are included in our empirical force field. It is of particular interest that the possible presence of π-electron delocalization in the $-C\begin{smallmatrix}O\\O\end{smallmatrix}$ group is manifested in the very high positive values of the CO-str./CO-str. and CO-str./OCO-bend interaction force constants (see the values of k_s and $f_{s\theta}$ in Table 9). Similarly large values for such types of interaction force constants have been reported for the formate [30], acetate [2], pyruvate [3], and propionate [5] ions.

iii) The effect of hydrogen bonding in this molecule may be reflected particularly in force constants associated with the $-CO_2$ and $-NH_3$ groups. For example, the diagonal force constants H_γ, H_{τ_1}, and H_{τ_2}, corresponding to the CO_2 in-plane rocking, CO_2- and NH_3-torsional coordinates, have the respective large values of 5.5312×10^{-9}, 0.6650×10^{-9}, and 0.6793×10^{-9} N nm.

iv) Since the two oxygen atoms in the carboxylate group are significantly out of the NCC plane, it is necessary to take into account particular interaction force constants of the in-plane CO_2-rocking (γ) and CO_2-deformational (θ) coordinates with several (quasi-A'') coordinates such as CH_2-twisting and -rocking coordinates. A detailed search for a set of such interaction force constants allowed us to choose two particular parameters, $h_{\gamma s_t}$ and $h_{\theta s_t}$. Removal of these force constants with a subsequent force field refinement led to a drastic increase in rms deviation to 6.0 cm^{-1} from its initial 3.32 cm^{-1}. This result indicates that the interaction constants of the CH_2-twisting coordinate with the CO_2 in-plane rocking and CO_2 deformational coordinates play an important role in reproducing the observed frequencies. These interactions are appreciable in the PED for the glycine isotopomers (cf. Table 1–4) in which strong couplings between the methylene twisting and CO_2 in-plane rocking modes are particularly evident.

Concluding Remarks

In this paper we have presented IR fundamental frequency data for 14 isotopomers of α-glycine. The fine structure of complex overlapping regions was revealed by measuring the spectra at 80 K. The low temperature measurement in combination with heavy atom (^{13}C, ^{15}N, and ^{18}O) isotopic shifts were often useful in elucidating vibrational assignments for some fundamentals of α-glycine. A total of 307 frequency data over the 14 isotopic species allowed us to determine a set of force constants constructing an empirical potential function for α-glycine. In spite of our considerable success in reproducing the observed frequencies, the reported description of the molecular motions in the normal modes in terms of a potential energy distribution remains somewhat uncertain since our empirical force field contains no intermolecular force terms. None the less, the present empirical force field, which is certainly much more reliable than earlier ones, should be helpful in future studies of the vibrational spectra of glycine.

Acknowledgements

The authors would like to express their thanks to Professor Kumao Hisano and Dr. Hirokazu Tanaka for their helpful advice. Numerical calculations were made in the Computer Center of the National Defense Academy by use of a HITAC M-200 H computer. This work was partially supported by a grant-in-aid for scientific research from the Kato Scientific Promotion Society.

[1] M. Kakihana, M. Kotaka, and M. Okamoto, J. Phys. Chem. **86,** 4385 (1982).
[2] M. Kakihana, M. Kotaka, and M. Okamoto, J. Phys. Chem. **87,** 2526 (1983).
[3] M. Kakihana and M. Okamoto, J. Phys. Chem. **88,** 1797 (1984).
[4] M. Kakihana and T. Nagumo, Z. Naturforsch. **42a,** 477 (1987).
[5] M. Kakihana and M. Akiyama, J. Phys. Chem. **91,** 4701 (1987).
[6] H. Hollenstein and H. H. Günthard, J. Mol. Spectrosc. **84,** 457 (1980).
[7] S. Suzuki, T. Shimanouchi, and M. Tsuboi, Spectrochim. Acta **19,** 1195 (1963).
[8] S. A. S. Ghazanfar, D. V. Myers, and J. T. Edsall, J. Amer. Chem. Soc. **86,** 3439 (1964).
[9] R. K. Khanna, M. Horak, and E. R. Lippincott, Spectrochim. Acta **22,** 1759 (1966).
[10] I. Laulicht, S. Pinchas, D. Samuel, and I. Wassermann, J. Phys. Chem. **70,** 2719 (1966).

[11] U. Stahlberg and E. Steger, Spectrochim. Acta **23 A,** 475 (1967).
[12] B. Dupuy and C. Garrigou-Lagrange, J. Chim. Phys. **65,** 1510 (1968).
[13] C. Destrade, C. Garrigou-Lagrange, and M. T. Forell, J. Mol. Struct. **10,** 203 (1971).
[14] J. F. Pearson and M. A. Slifkin, Spectrochim. Acta **28 A,** 2403 (1972).
[15] A. M. Dwivedi and V. D. Gupta, Ind. J. Biophys. **10,** 77 (1973).
[16] H. S. Randhawa and C. N. R. Rao, J. Cryst. Mol. Struct. **3,** 309 (1973).
[17] H. Stenbäck, J. Raman Spectrosc. **5,** 49 (1976).
[18] K. Machida, A. Kagayama, Y. Saito, Y. Kuroda, and T. Uno, Spectrochim. Acta **33 A,** 569 (1977).
[19] K. Machinda, A. Kagayama, and Y. Kuroda, Bull. Chem. Soc. Jpn. **54,** 1348 (1981).
[20] H. Baba, A. Mukai, T. Shimanouchi, and S. Mizushima, Nippon Kagaku Zasshi **70,** 333 (1949).
[21] P. G. Jönsson, Å. Kvick, Acta Cryst. **28 B,** 1827 (1972).
[22] L. F. Power, K. E. Turner, and F. H. Moore, Acta Cryst. **32 B,** 11 (1976).
[23] L. J. Bellamy, The Infrared Spectra of Complex Molecules. – Advances in Infrared Group Frequencies, 2nd ed., Chapman and Hall, New York 1980, Vol. 2.
[24] D. M. Byler and H. Susi, Spectrochim. Acta **35 A,** 1365 (1979).
[25] H. Susi and D. M. Byler, J. Mol. Struct. **63,** 1 (1980).
[26] M. Kakihana, unpublished data.
[27] E. B. Wilson, Jr., J. C. Decius, and P. C. Cross, Molecular Vibrations. McGraw-Hill: New York 1955.
[28] H. Hollenstein and H. H. Günthard, Chem. Phys. **4,** 368 (1974).
[29] H. Hollenstein, R. W. Schär, N. Schwizgebel, G. Grasssi, and H. H. Günthard, Spectrochim. Acta **39 A,** 193 (1983).
[30] K. G. Kidd and H. H. Mantsch, J. Mol. Spectrosc. **85,** 375 (1981).